Bistable nanoelectromechanical devices

Kirk J. Ziegler, Daniel M. Lyons, and Justin D. HolmesDonats Erts and Boris PolyakovHåkan Olin, Krister Svensson, and Eva Olsson

Citation: Appl. Phys. Lett. **84**, 4074 (2004); doi: 10.1063/1.1751622
View online: http://dx.doi.org/10.1063/1.1751622
View Table of Contents: http://aip.scitation.org/toc/apl/84/20
Published by the American Institute of Physics

Bistable nanoelectromechanical devices

Kirk J. Ziegler, Daniel M. Lyons, and Justin D. Holmes[a)]
Department of Chemistry, Materials Section and Supercritical Fluid Centre, University College Cork, Cork, Ireland

Donats Erts and Boris Polyakov
Institute of Chemical Physics, University of Latvia, LV-1586 Riga, Latvia

Håkan Olin,[b)] Krister Svensson, and Eva Olsson
Physics and Engineering Physics, Chalmers University of Technology, SE-412 96 Göteborg, Sweden

(Received 19 January 2004; accepted 23 March 2004; published online 5 May 2004)

A combined transmission electron microscopy-scanning tunneling microscopy (TEM-STM) technique has been used to investigate the force interactions of silicon and germanium nanowires with gold electrodes. The $I(V)$ data obtained typically show linear behavior between the gold electrode and silicon nanowires at all contact points, whereas the linearity of $I(V)$ curves obtained for germanium nanowires were dependent on the point of contact. Bistable silicon and germanium nanowire-based nanoelectromechanical programmable read-only memory (NEMPROM) devices were demonstrated by TEM-STM. These nonvolatile NEMPROM devices have switching potentials as low as 1 V and are highly stable making them ideal candidates for low-leakage electronic devices.
 [DOI: 10.1063/1.1751622]

Bottom-up assembly of well-defined nanoscale building blocks, such as molecules, quantum dots, and nanowires, represents a powerful approach for the construction of future integrated circuits. Indeed, some researchers have already demonstrated that semiconductor nanowires and carbon nanotubes can act as building blocks for the assembly of simple devices and interconnects.[1] Although the optical and electronic properties of nanotubes and nanowires have been intensely investigated, there have been few studies on the force interactions of nanotubes[2,3] and no studies on the force interactions of nanowires with electrical contacts. Such studies are, however, important parameters to investigate in the development of nanoelectromechanical systems (NEMS). Traditionally, mechanical devices are considered to be slow. However, utilizing nanoscale structures for mechanical devices could in theory achieve GHz or THz resonance frequencies making NEMS faster than current electronic devices.[3,4] To date, researchers have focused on using carbon nanotubes as building blocks for the construction of NEMS due to their mechanical strength.[4,5] However, during carbon nanotube synthesis both metal and semiconducting nanotubes are generated rendering the electrical response of nanodevices based on carbon nanotubes unpredictable. Semiconductor nanowires, such as silicon or germanium, however, offer the distinct advantage over carbon nanotubes in that their sizes and electronic properties can be controlled in a predictable manner during their synthesis.[6] Thus, the electrical response of NEMS based on semiconductor or metallic nanowires should be more predictable than carbon nanotube based devices and have recently been investigated.[7]

The combination of transmission electron microscopy (TEM) with scanning tunneling microscopy (STM) (TEM-STM) allows direct visualization of the materials being investigated.[8] In this letter, we describe an *in situ* TEM-STM probing technique to measure the force interactions of silicon and germanium nanowires with gold electrodes. The jump-to-contact and jump-off-contact distances of the nanowires to and from the electrode were measured to determine the van der Waals (vdW) and electrostatic force interactions important to the development of NEMS. We also illustrate how the semiconductor nanowires can be utilized in the construction of a simple nanoelectromechanical programmable read-only memory (NEMPROM) device.

Silicon and germanium nanowires were synthesized directly onto a macroscopic gold wire (diameter$=0.25$ mm) which was subsequently used in the TEM-STM experiments (see EPAPS Ref. 9 for supplemental material) as shown in Fig. 1. The controlled approach of the electrode to the nanowire was utilized to measure the distance at which the nanowire jumped to the gold contact (jump-to-contact distance). After contact of the nanowire with the gold electrode, controlled withdrawal of the piezotube resulted in nanowire/contact separation and a measurable jump-off-contact distance. The jump-to-contact and jump-off-contact distances were measured at different applied voltages and can be directly related to the attractive forces between the nanowire tip and the gold electrode as demonstrated in Fig. 1(b). The attractive vdW forces (F_{vdW}) and electrostatic interactions (F_{elec}) between the nanowire and the gold electrode are countered by the opposing elastic energy (F_{elas}) exerted by the nanowire. The pull-on and pull-off forces between the nanowire and the Au electrode can be calculated using the spring constant of the nanowires, k.

To relate the vdW and electrostatic forces to the pull-on and pull-off forces, the total force (F_T) acting on the nanowire was calculated at different applied voltages assuming that the total force is the sum of vdW and electrostatic interactions, $F_T = F_{\mathrm{vdW}} + F_{\mathrm{elec}}$. Although the attractive interac-

a)Electronic mail: j.holmes@ucc.ie
b)Present address: Department of Engineering Physics and Mathematics, Mid Sweden University, SE-85170 Sundsvall, Sweden.

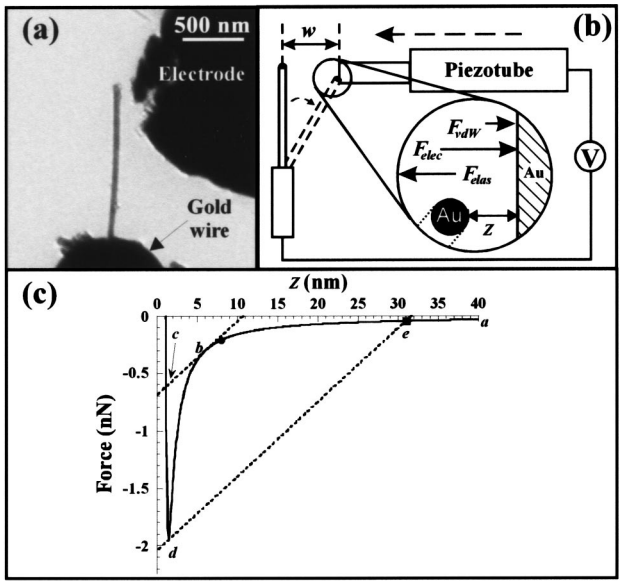

FIG. 1. (a) TEM image of a Ge nanowire utilized for TEM-STM measurements. (b) Schematic representation of TEM-STM studies. The electrode is positioned by movement of the piezotube. The zoom-in schematic demonstrates the force interactions between the Si or Ge nanowire tip and the electrode where z is the distance of separation between the nanowire tip and the electrode with w being the initial separation distance. The attractive vdW (F_{vdW}) and electrostatic (F_{elec}) forces are countered by the elastic force exerted by the nanowire (F_{elas}). With applied electrostatic voltages, the total force acting on the nanowire tip is $F_T = F_{\mathrm{vdW}} + F_{\mathrm{elec}}$. (c) Force–distance plot calculated for the interactions of a Si nanowire ($d = 90$ nm) with an applied voltage of 1 V. The dotted lines represent the spring constant of the nanowire. Measured jump-to-contact (circle) and jump-off-contact (square) distances are plotted for comparison.

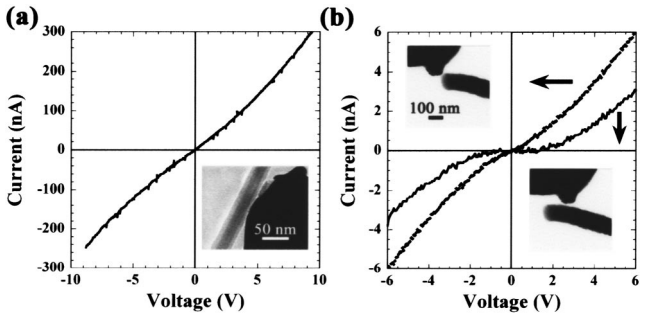

FIG. 2. Characteristic $I(V)$ behavior for an individual (a) Si or (b) Ge nanowire. Note that the $I(V)$ for Ge nanowires are contact dependent.

tions will be a function of geometry, we found that a sphere (wire)-plane (electrode) geometry, commonly used in AFM studies,[10,11] gave the most accurate results [see zoom-in schematic of Fig. 1(b)]. Combining the vdW and electrostatic forces (see EPAPS Ref. 9) between the tip of a Si nanowire ($d = 91$ nm) and the gold electrode results in force–distance curves typical to that shown in Fig. 1(c) for an electrostatic potential of 1 V. As the nanowire tip is moved toward the electrode (point *a*), the attractive forces acting on the nanowire tip steadily increase. At point *b*, the attractive force gradient exceeds the spring constant (dotted lines) of the nanowire ($dF_T/dz \geqslant dF_{\mathrm{elas}}/dz = k$)[10] and the physical jump-to-contact occurs and comes to equilibrium at the intersection of $F(z)$ and the spring constant (point *c*). The jump-to-contact distance is the distance between points *b* and *c* and varies from AFM jump-to-contact distances because the tip and sample deflection can be viewed in our experiments. The jump-off-contact occurs once the spring constant is greater than the total attractive force gradient ($dF_T/dz \leqslant dF_{\mathrm{elas}}/dz = k$), which occurs at the minimum in the force curve (point *d*). The calculated jump-off-contact distances (point *e*) were determined from the spring constant and the minimum in the force–distance curve.[12] There is agreement between the calculations and the experimental results of the jump-to-contact distance at low voltages ($V \leqslant 1$). At higher voltages ($V > 1$), the experimentally determined jump-to-contact distances were longer than calculated. This discrepancy suggests that the electrostatic attractive forces are stronger than the theoretical sphere–plane interactions calculated at high potentials possibly due to the breakdown of the electrostatic potential equation at high voltages or large distances[12] or due to error in the calculated spring constant. The jump-off-contact distances predicted are also in agreement with the experimental results at low voltages ($V \leqslant 1$). However, at higher voltages substantially shorter experimental jump-off-contact distances are observed than predicted by the calculations. These discrepancies are possibly due to shearing forces that occur at the nanowire/electrode contact during nanowire withdrawal minimizing adhesion forces and resulting in shorter jump-off-contact distances.

Si nanowires (40–90 nm in diameter) typically displayed linear $I(V)$ behavior as shown in Fig. 2(a), and was independent of the point of contact between the nanowire and the gold electrode. The resistance of the Si nanowires did not vary significantly with contact area when the contact width was changed between 4 and 55 nm resulting in resistances between 15 and 45 MΩ. Although the contact resistances cannot be adequately determined through simple two-point contact, the resistivities of the Si nanowires can be approximated to be of the order of 10^{-2} Ω m. The relatively low resistivities for Si nanowires are indicative of a highly doped nanowire with an impurity concentration of approximately 10^{16} cm^{-3}.[13] Ge nanowires (40–150 nm in diameter) showed $I(V)$ curves that were dependent on the point of contact as seen in Fig. 2(b). Contact through the side of the nanowire showed a nonconductive gap, which varied randomly (1–8 V) but typically was between 2 and 4 V. However, moving the electrode to the nanowire tip and contacting the gold hemisphere typically resulted in a significant decrease in the nonconductive gap and in nearly linear $I(V)$ behavior. These changes in the $I(V)$ behavior with contact position suggest that there is an unstable native oxide layer on the Ge nanowires of varying thickness which acts as a barrier to the conductance. The resistance of the Ge nanowires varied significantly between 0.15 and 1 GΩ corresponding to resistivities of the order of 10^{-1} Ω m. The higher resistivity suggests that the Ge nanowires are not as highly doped with gold as the Si nanowires having an impurity concentration of approximately 10^{14} cm^{-3}.[13]

These semiconductor nanowires were utilized for the development of NEMS, such as nanoelectromechanical programmable read-only memory (NEMPROM) devices, which require two stable conditions (ON/OFF). To quantify the bistability behavior of nanowire-based NEMPROM devices, calculations based on the total potential energy of the nanowire $E_T = E_{\mathrm{vdW}} + E_{\mathrm{elec}} + E_{\mathrm{elas}}$ were performed. The vdW and electrostatic potentials were calculated using the relation-

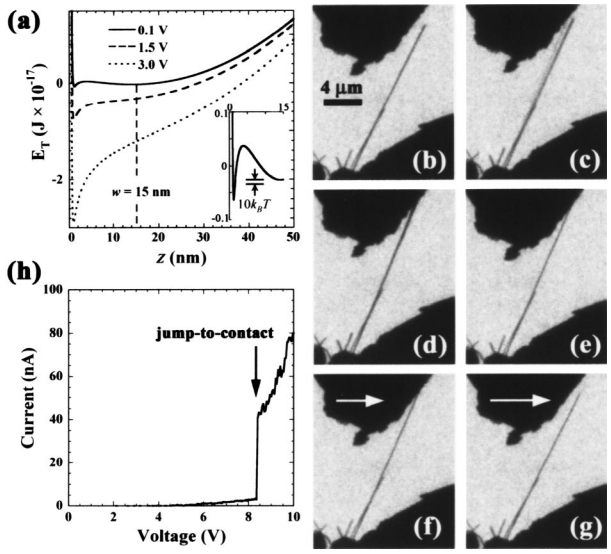

FIG. 3. (a) NEMPROM device calculations at different electrostatic potentials for Ge nanowire ($d=50$ nm; $l=1.5$ μm). Inset shows the energy barrier between the two stable (ON/OFF) minima in relation to $10k_BT$. (b)–(d) TEM sequence showing the jump-to-contact of a Ge nanowire as the voltage is increased. (e) TEM image demonstrating the stability of device after removal of the electrostatic potential. (f) and (g) TEM sequence demonstrating the resetting behavior of the device. Note that the device is indefinitely stable but reset with a slight amount of shearing motion. (h) $I(V)$ of NEMPROM device showing no conductivity until after contact is made at a potential of 8.4 V.

ships described above where $E=\int F dz$. The switching behavior of a Ge nanowire-based NEMPROM device is seen in Fig. 3. Figure 3(a) shows the calculated potential energy diagrams for the nanowire–electrode interactions. There are two local minima (~1 and ~15 nm) at low voltages and the circuit is initially OFF due to the energy minimum at the device separation distance (w) where the elastic energy of the nanowire is minimal. The other minimum (ON) is due to vdW interactions when the wire and electrode are in contact. To switch between these two minima, an electrostatic field of 3 V is applied which alters the interaction energy resulting in the deflection of the nanowire into contact with the gold electrode producing an ON state. Removal of the electrostatic potential, however, does not allow the nanowire to switch back to the OFF position due to the energy barrier $(\gg 10k_BT)$[4] between the two local minima at low voltage [see the inset of Fig. 3(a)].

An example of a NEMPROM device made from a Ge nanowire is shown in the TEM sequence of Figs. 3(b)–3(g). As the voltage is slowly increased in Figs. 3(b) and 3(c), the device remains OFF. However, once the voltage is increased to 8.4 V, jump-to-contact is made as seen in Fig. 3(d) and in the $I(V)$ in Fig. 3(h). The jump-to-contact is too fast to be measured but the resonant frequency of this nanowire can be estimated to be in the MHz regime. The nanowire remains in contact (ON) with the electrode even when the electrostatic field is removed due to the minimum in the potential energy curve [Fig. 3(e)]. These devices remain indefinitely stable demonstrating the nonvolatility of these devices for memory applications or other low-leakage devices. Although these devices are highly stable, these NEMPROM devices can be switched OFF by mechanical motion or by heating the device above the stability limit $(\gg 10k_BT)$. Figures 3(e) through 3(g) demonstrate that little shearing motion is required to overcome the vdW attractive forces. The relatively large switching potential utilized in this device was used for demonstration purposes so that the full deflection of the nanowire could be easily viewed. Smaller separation distances require much smaller switching potentials. However, there is a minimum distance or critical gap [point *b* of Fig. 1(c)] that must be maintained or the device will become unstable due to the strong vdW attractive forces resulting in the formation of a single minimum. NEMPROM devices can function at any distance between points *b* and *e* of the force–distance curve in Fig. 1(c). The NEMPROM devices synthesized in our experiments were robust; each nanowire tested could be switched ON and OFF multiple times (20–50) without noticeable deformation or fracture. However, further experimentation is required to determine their viability in future devices.

The authors would like to thank Lars Ryen for assistance with the TEM, Heinrich Riedl for his assistance, and Michael A. Morris for useful discussions. We acknowledge financial support from Enterprise Ireland for a postdoctoral fellowship for K.J.Z., the Higher Education Authority (HEA) Ireland, the Council of Science of Latvia, and the University of Latvia.

[1] Y. Cui and C. M. Lieber, Science **291**, 851 (2001); X. Duan, Y. Huang, and C. M. Lieber, Nano Lett. **2**, 487 (2002); Y. Huang, X. Duan, Y. Cui, L. J. Lauhon, K.-H. Kim, and C. M. Lieber, Science **294**, 1313 (2001); S. J. Tans, A. R. M. Verschueren, and C. Dekker, Nature (London) **393**, 49 (1998); R. Martel, T. Schmidt, H. R. Shea, T. Hertel, and P. Avouris, Appl. Phys. Lett. **73**, 2447 (1998); S.-W. Chung, J.-Y. Yu, and J. R. Heath, *ibid.* **76**, 2068 (2000).
[2] M. Duquesnes, S. V. Rotkin, and N. R. Aluru, Nanotechnology **13**, 120 (2002); K. A. Bulashevich and S. V. Rotkin, JETP Lett. **75**, 205 (2002).
[3] J. M. Kinaret, T. Nord, and S. Viefers, Appl. Phys. Lett. **82**, 1287 (2003).
[4] T. Rueckes, K. Kim, E. Joselevich, G. Y. Tseng, C.-L. Cheung, and C. M. Lieber, Science **289**, 94 (2000).
[5] P. Poncharal, Z. L. Wang, D. Ugarte, and W. A. de Heer, Science **283**, 1513 (1999); N. R. Franklin, Q. Wang, T. W. Tombler, A. Javey, M. Shim, and H. Dai, Appl. Phys. Lett. **81**, 913 (2002); L. Pescini, H. Lorenz, and R. H. Blick, *ibid.* **82**, 352 (2003); P. Kim and C. M. Lieber, Science **286**, 2148 (1999).
[6] Y. Xia, P. Yang, Y. Sun, Y. Wu, B. Mayers, B. Gates, Y. Yin, F. Kim, and H. Yan, Adv. Mater. (Weinheim, Ger.) **15**, 353 (2003).
[7] H. Yamaguchi and Y. Hirayama, Surf. Sci. **532–535**, 1171 (2003); A. Husain, J. Hone, H. W. C. Postma, X. M. H. Huang, T. Drake, M. Barbic, A. Scherer, and M. L. Roukes, Appl. Phys. Lett. **83**, 1240 (2003).
[8] H. Ohnishi, Y. Kondo, and K. Takayanagi, Nature (London) **395**, 780 (1998); D. Erts, H. Olin, L. Ryen, E. Olsson, and A. Tholen, Phys. Rev. B **61**, 12725 (2000); T. Kizuka, Phys. Rev. Lett. **81**, 4448 (1998).
[9] See EPAPS Document No. E-APPLAB-84-052420 for experimental and calculation details. A direct link to this document may be found in the online article's HTML reference section. The document may also be reached via the EPAPS homepage (http://www.aip.org/pubservs/epaps.html) or from ftp.aip.org in the directory/epaps/. See the EPAPS homepage for more information.
[10] B. Cappella and G. Dietler, Surf. Sci. Rep. **34**, 1 (1999).
[11] L. Olsson, N. Lin, V. Yakimov, and R. Erlandsson, J. Appl. Phys. **84**, 4060 (1998).
[12] H. W. Hao, A. M. Baro, and J. J. Saenz, J. Vac. Sci. Technol. B **9**, 1323 (1991).
[13] S. M. Sze, *Physics of Semiconductor Devices*, 2nd ed. (Wiley-Interscience, New York, 1981).